Synthesis of Variable-Sized Nanocrystals of Fe_3O_4 with High Surface Reactivity

Daniela Caruntu,[†] Gabriel Caruntu,[†] Yuxi Chen,[†] Charles J. O'Connor,*[,†] Galina Goloverda,[‡] and Vladimir L. Kolesnichenko*[,‡]

Advanced Materials Research Institute, University of New Orleans, New Orleans, Louisiana 70148, and Department of Chemistry, Xavier University of Louisiana, New Orleans, Louisiana 70125

Received July 23, 2004. Revised Manuscript Received August 30, 2004

A new rational method of synthesis of nanocrystalline iron (II, III) oxide is based on the elevated-temperature hydrolysis of chelate iron alkoxide complexes in solutions of corresponding alcohol, diethylene glycol, and *N*-methyl diethanolamine. The rates of reaction and crystallization are easily tuned by varying the concentration of reactants and changing the temperature. The size of the nanocrystals is controlled by changing the complexing strength of the reaction medium: 5.7 nm in diethylene glycol, 16.8 nm in *N*-methyl diethanolamine, and 12.7 nm in a 1:1 mixture of both solvents. The nanocrystalline powdered Fe_3O_4 products were isolated with a high yield. The surface of the obtained nanocrystals is passivated by molecules of adsorbed donating solvent that provide stability against agglomeration, provide solubility in polar protic solvents (water and methanol), and allow reactions at the nanocrystal surface.

Introduction

Nanocrystalline metal oxides are generally synthesized by a variety of methods based on relatively simple chemical reactions yielding products with desired composition, purity, and crystal structure. Obtaining the nanocrystals with variable and uniform size is a significant challenge, however, because controlling the crystal growth in all of its steps is not so easy to accomplish. Many common methods are rooted in the ion metathesis reactions in solution. These straightforward reactions provide good yield and purity of the products, but they occur instantly on mixing and leave little possibility to control the course of the crystallization. Different techniques were developed to address this problem. According to one of them, ion metathesis reactions are performed under strictly controlled conditions of mixing such as addition of the dilute reactant solutions at a restricted rate with vigorous stirring and maintaining the proper temperature.[1] The nanocrystal growth is controlled also by performing metathesis reactions in heterogeneous media of microemulsions where aqueous micelles of variable sizes act as microreactors.[2] In a third method, the precipitating agent (OH^-) is slowly generated in aqueous solution by hydrolysis of a molecular precursor (urea, urotropin, etc.).[3] The greatest advantage of these techniques is that the surface of the produced nanocrystals remains active and available for postsynthesis chemical modification.

Other methods use the nucleophilic property of water in hydrolysis of metal precursors. Reactions usually are slower than ion metathesis reactions, and therefore crystallization is easier to control. Hydrolyzable salts of metal ions are used for synthesis of corresponding oxides in colloidal form by their forced hydrolysis under hydrothermal conditions[4] or in high-boiling solvents (polyols).[5] Hydrolysis in nonaqueous solutions has been applied also to metal alkoxides[6] and β-diketonates,[7] offering a convenient route to the uncapped nanoparticles.

* Corresponding author. E-mail: vkolesni@xula.edu; coconnor@uno.edu.

[†] University of New Orleans.

[‡] Xavier University of Louisiana.

(1) (a) Kang, Y. S.; Risbud, S.; Rabolt, J. F.; Stroeve, P. *Chem. Mater.* **1996**, *8*, 2209. (b) Kim, D. K.; Mikhaylova, M.; Zhang, Y.; Muhammed, M. *Chem. Mater.* **2003**, *15*, 1617. (c) McKenzie, K. J.; Marken, F. *Pure Appl. Chem.* **2001**, *73*, 1885. (d) Sousa, M. H.; Tourinho, F. A.; Depeyrot, J.; da Silva, G. J.; Lara, M. C. F. L. *J. Phys. Chem. B* **2001**, *105*, 1168. (e) Aquino, R.; Tourinho, F. A.; Itri, R.; e Lara, M. C. F. L.; Depeyrot, J. *J. Magn. Magn. Mater.* **2002**, *252*, 23. (f) Zaitsev, V. S.; Filimonov, D. S.; Presnyakov, I. A.; Gambino, R. J.; Chu, B. *J. Colloid Interface Sci.* **1999**, *212*, 49. (g) Babes, L.; Denizot, B.; Tanguy, G.; Le Jeune, J. J.; Jallet, P. *J. Colloid Interface Sci.* **1999**, *212*, 474. (h) Sauzedde, F.; Elaïssari, A.; Pichot, C. *Colloid Polym. Sci.* **1999**, *277*, 846. (i) Marquez, M.; Robinson, J.; Van Nostrand, V.; Schaefer, D.; Ryzhkov, L. R.; Lowe, W.; Suib, S. L. *Chem. Mater.* **2002**, *14*, 1493.

(2) (a) Pileni, M. P.; Lisiecki, I.; Motte, L.; Petit, C.; Tanori, J.; Moumen, N. In *Micelles, Microemulsions, Monolayers*; Shah, D. O., Ed.; Dekker: New York, 1998; p 289. (b) Pileni, M. P.; Feltin, N.; Moumen, N. In *Scientific and Clinical Applications of Magnetic Carriers*; Haefeli, U., Ed.; Plenum Press: New York, 1997; p 117. (c) Hochepied, J. F.; Bonville, P.; Pileni, M. P. *J. Phys. Chem. B* **2000**, *104*, 905. (d) Rondinone, A. J.; Samia, A. C. S.; Zhang, Z. J. *J. Phys. Chem. B* **1999**, *103*, 6876. (e) Rondinone, A. J.; Samia, A. C. S.; Zhang, Z. J. *J. Phys. Chem. B* **2000**, *104*, 7919. (f) Liu, C.; Zou, B.; Rondinone, A. J.; Zhang, Z. J. *J. Am. Chem. Soc.* **2000**, *122*, 6263.

(3) (a) Ocana, M.; Morales, M. P.; Serna, C. J. *J. Colloid Interface Sci.* **1999**, *212*, 317. (b) Ocana, M.; Matijevic, E. *J. Mater. Res.* **1990**, *5*, 1083. (c) Verges, M. A.; Mifsud, A.; Serna, C. J. *J. Chem. Soc., Faraday Trans.* **1990**, *86*, 959.

(4) (a) Morales, M. P.; Gonzalez-Carreno, T.; Serna, C. J. *J. Mater. Res.* **1992**, *7*, 2538. (b) Matijevic, E.; Sapieszko, R. S. *Surf. Sci. Ser.* **2000**, *92*, 2. (c) Blesa, M. A.; Matijevic, E. *Adv. Colloid Interface Sci.* **1989**, *29*, 173.

(5) (a) Feldmann, C. *Adv. Mater.* **2001**, *13*, 1301. (b) Feldmann, C. *Adv. Funct. Mater.* **2003**, *13*, 101. (c) Feldmann, C.; Jungk, H.-O. *Angew. Chem., Int. Ed.* **2001**, *40*, 359. (d) Ammar, S.; Helfen, A.; Jouini, N.; Fiévet, F.; Rosenman, I.; Villain, F.; Molinié, P.; Danot, M. *J. Mater. Chem.* **2001**, *11*, 186. (e) Rajamathi, M.; Ghosh, M.; Seshadri, R. *Chem. Commun.* **2002**, 1152.

10.1021/cm0487977 CCC: $27.50
Published on Web 11/11/2004

A different synthetic approach replaces the hydrolysis or ion metathesis reactions by thermal decomposition of oxygen-rich molecular precursors or metal carbonyls in the presence of oxygen or oxygen donors in solutions of high-boiling nonpolar solvents.[8] This technique offers a convenient way to manipulate the kinetics of crystallization and therefore the nanocrystal dispersity. The thermal decomposition technique is usually used in conjunction with tactical targeting control over composition of the surface of growing nanocrystals. The synthesis reactions are performed in the presence of complexing agents that reversibly bind to the coordinatively unsaturated metal atoms at the crystal surface. These complexing agents (capping ligands) contain one or more substituents that provide steric separation between nanocrystals and adjust their affinity to the medium, stabilizing their colloids. Capping ligands[9] and coordinating polymers[10] are sometimes used also to passivate the nanocrystal surface in combination with hydrolytic and ion metathesis methods.

In this paper, we describe a new method for synthesis of the nanocrystalline metal oxides that is based on the hydrolysis of chelate metal alkoxide complexes at elevated temperature in solutions of the parent chelating alcohols. This method allows the preparation of nonaggregated nanocrystals with variable size and composition and high crystallinity. The surface of the isolated nanoparticles is coated with a labile layer of the solvent and remains chemically active and available for further derivatization. Nanocrystals in this state are capable of forming stable aqueous colloids without using capping ligands or surfactants. The developed method represents a highly economical and facile "green" process that can be used for scaled preparations. This method may contribute to the development of new catalysts, functional magnetic and optoelectronic materials, and biocompatible magnetic materials for their application in biology and medicine as diagnostic and therapeutic tools.

Experimental Section

Chemicals. The reagents and solvents were purchased from the following companies: iron(III) chloride hexahydrate 97%, toluene 99.5%, methyl alcohol 99.8%, and hexanes 98.5% from Merck; diethylene glycol 99%, *N*-methyl diethanolamine 99+%, sodium hydroxide 97% (20−40 mesh beads), ethyl acetate 99.5%, and decane 99+% from Aldrich; iron(II) chloride tetrahydrate 99% from Alfa Aesar; oleic acid 90% from Fisher; and absolute ethanol from AAper Alcohol and Chemical Co. Chemicals and solvents were used without further purification. The air-sensitive chemicals were manipulated in a VAC glovebox with a nitrogen atmosphere.

Synthesis. All syntheses were carried out using the Schlenk technique under argon atmosphere.

Preparation of Magnetite Nanoparticles in Diethylene Glycol. A 2 mmol amount of $FeCl_2 \cdot 4H_2O$ and 4 mmol of $FeCl_3 \cdot 6H_2O$ were dissolved in 80 g of diethylene glycol (DEG) in a Schlenk flask under protection with argon. Separately, 16 mmol of NaOH was dissolved in 40 g of diethylene glycol. The solution of NaOH was added to the solution of metal chlorides with stirring at room temperature, causing an immediate color change from yellow-brown to deep green-brown. After 3 h, the temperature of solution was raised during 1.5 h to 210 °C and then kept constant for 2 h in the temperature range 210−220 °C. The solid product was isolated by cooling the reaction mixture to room temperature and centrifuging. A black solid was obtained and washed with ethanol twice and with a mixture of ethanol and ethyl acetate (1:1, v/v) three times to remove the excess of diethylene glycol and was dried in a flow of nitrogen. The typical yield was 95−96%. When reactivity tests or the preparation of colloids were planned, the solids were used without drying.

To obtain iron oxide nanoparticles soluble in nonpolar solvents, a diethylene glycol solution of oleic acid (2.6 mmol of oleic acid per 20 g of DEG) was added to the reaction mixture at high temperature. This addition immediately precipitated the solids. The mixture was cooled to room temperature and then centrifuged. The precipitates were washed with methanol and dissolved in 20 mL of toluene. The resulting solution was centrifuged and mixed with 2−3 volumes of methanol. The precipitate was separated by centrifuging, washed with methanol, and kept either moistened with methanol or dispersed in nonpolar solvents (hexanes, toluene, and decane).

Preparation of Magnetite Nanoparticles in a Mixture of Diethylene Glycol and *N*-Methyl Diethanolamine (1:1, w/w). A 2 mmol amount of $FeCl_2 \cdot 4H_2O$ and 4 mmol of $FeCl_3 \cdot 6H_2O$ were dissolved in 40 g of diethylene glycol in a Schlenk flask under argon. When the salts were completely dissolved, 40 g of *N*-methyl diethanolamine was added, and the solution immediately turned from yellow-brown to deep brown-green. The resulting solution was stirred for 1 h at room temperature. Separately, 16 mmol of NaOH was dissolved in 20 g of diethylene glycol and then mixed with 20 g of *N*-methyl diethanolamine. The solution of NaOH was added to the solution of metal chlorides with stirring at room temperature, causing an immediate color change from deep green-brown to deep green. After 3 h, the temperature of solution was raised during 1.5 h to 210 °C and then kept constant for 3 h in the temperature range 210−220 °C. After the solution was cooled, the solid product was isolated by centrifuging, washing with ethanol twice and with a mixture of ethanol and ethyl acetate (1:1, v/v) three times, and drying in a flow of nitrogen. The typical isolated yield of black powders was 80−90% (for products containing 96−97% of metal oxide).

Magnetite nanoparticles soluble in nonpolar solvents were obtained by heating to reflux for 0.5−1 h a mixture containing 80 mg of black powder and a toluene solution of oleic acid (0.5 mmol of oleic acid per 25 mL of toluene). A deep brown solution

(6) (a) Liu, C.; Zou, B.; Rondinone, A. J.; Zhang, Z. J. *J. Am. Chem. Soc.* **2001**, *123*, 4344. (b) O'Brien, S.; Brus, L.; Murray, C. B. *J. Am. Chem. Soc*. **2001**, *123*, 12085.

(7) (a) Broussous, L.; Santilli, C. V.; Pulcinelli, S. H.; Craievich, A. F. *J. Phys. Chem.* **2002**, *106*, 2855. (b) Grosso, D.; Sermon, P. *J. Mater. Chem.* **2000**, *10*, 359. (c) Gamard, A.; Babot, O.; Jousseaume, B.; Rascle, M.-C.; Toupance, T.; Campet, G. *Chem. Mater.* **2000**, *12*, 3419. (d) de Monredon, S.; Cellot, A.; Ribot, F.; Sanchez, C.; Armelao, L.; Gueneau, L.; Delattre, L. *J. Mater. Chem.* **2002**, *12*, 2396.

(8) (a) Rockenberger, J.; Scher, E. C.; Alivisatos, A. P. *J. Am. Chem. Soc*. **1999**, *121*, 11595. (b) Seo, W. S.; Jo, H. H.; Lee, K.; Park, J. T. *Adv. Mater*. **2003**, *15*, 795. (c) Thimmaiah, S.; Rajamathi, M.; Singh, N.; Bera, P.; Meldrum, F.; Chandrasekhar, N.; Seshadri, R. *J. Mater. Chem.* **2001**, *11*, 3215. (d) Sun, S.; Zeng, H.; Robinson, D. B.; Raoux, S.; Rice, P. M.; Wang, S. X.; Li, G. *J. Am. Chem. Soc*. **2004**, *126*, 273. (e) Hyeon, T.; Lee, S. S.; Park, J.; Chung, Y.; Na, H. B. *J. Am. Chem. Soc.* **2001**, *123*, 12798. (f) Bourlinos, A. B.; Simopoulos, A.; Petridis, D. *Chem. Mater*. **2002**, *14*, 899. (g) Trentler, T. J.; Denler, T. E.; Bertone, J. F.; Agrawal, A.; Colvin, V. L. *J. Am. Chem. Soc*. **1999**, *121*, 1613. (h) Boal, A. K.; Das, K.; Gray, M.; Rotello, V. M. *Chem. Mater*. **2002**, *14*, 2628. (i) Shafi, K. V. P. M.; Ulman, A.; Yan, X.; Yang, N.-L.; Estournès, C.; White, H.; Rafailovich, M. *Langmuir* **2001**, *17*, 5093. (j) Yin, M.; O'Brien, S. *J. Am. Chem. Soc*. **2003**, *125*, 10180. (k) Cozzoli, P. D.; Curri, M. L.; Agostiano, A.; Leo, G.; Lomascolo, M. *J. Phys. Chem. B* **2003**, *107*, 4756. (l) Cheon, J.; Kang, N.-J.; Lee, S.-M.; Lee, J.-H.; Yoon, J.-H.; Oh, S. J. *J. Am. Chem. Soc*. **2004**, *126*, 1950. (m) Li, Z.; Chen, H.; Bao, H.; Gao, M. *Chem. Mater*. **2004**, *16*, 1391.

(9) (a) Wakefield, G.; Keron, H. A.; Dobson, P. J.; Hutchison, J. L. *J. Colloid Interface Sci.* **1999**, *215*, 179. (b) Wong, E. M.; Hoertz, P. G.; Liang, C. J.; Shi, B.-M.; Meyer, G. J.; Searson, P. C. *Langmuir* **2001**, *17*, 8362. (c) Rajamathi, M.; Ghosh, M.; Seshadri, R. *Chem. Commun*. **2002**, 1152. (d) O'Brien, S.; Brus, L.; Murray, C. B. *J. Am. Chem. Soc*. **2001**, *123*, 12085. (e) Cozzoli, P. D.; Kornowski, A.; Weller, H. *J. Am. Chem. Soc*. **2003**, *125*, 14539.

(10) (a) Skoutelas, A. P.; Karakassides, M. A.; Petridis, D. *Chem. Mater*. **1999**, *11*, 2754. (b) Guo, L.; Yang, S.; Yang, C.; Yu, P.; Wang, J.; Ge, W.; Wong, G. K. L. *Chem. Mater*. **2000**, *12*, 2268. (c) Papisov, M. I.; Bogdanov, A., Jr.; Schaffer, B.; Nossiff, N.; Shen, T.; Weissleder, R. *J. Magn. Magn. Mater*. **1993**, *122*, 383.

was obtained, and the solid product was reprecipitated by adding 1−2 volumes of methanol and then washed several times with methanol to remove the excess of oleic acid. The precipitate was kept either moistened with methanol or dispersed in nonpolar solvents (hexanes, toluene, and decane).

Preparation of Magnetite Nanoparticles from *N*-Methyl Diethanolamine Solutions. A 2 mmol amount of $FeCl_2 \cdot 4H_2O$ and 4 mmol of $FeCl_3 \cdot 6H_2O$ were dissolved in 40 g of *N*-methyl diethanolamine in a Schlenk flask under protection of argon. Separately, 16 mmol of NaOH was dissolved in 40 g of *N*-methyl diethanolamine. A solution of NaOH was then added to a solution of metal chlorides while stirring at room temperature, causing an immediate color change from deep brown to deep green. After 3 h, the temperature of solution was raised during 1.5 h to 210 °C and then kept constant for 4 h in the temperature range 210−220 °C. The solid product was isolated by cooling the reaction mixture to room temperature and then centrifuging. A black solid was obtained and washed with ethanol twice and with a mixture of ethanol and ethyl acetate (1:1, v/v) three times and dried in a flow of nitrogen. The yield of black powder was 0.294 g (63%).

Characterization. The structure and phase purity of the nanopowders were investigated by X-ray diffractometry (XRD). The measurements were performed with a Phillips X'pert system equipped with a graphite monochromator (Cu Kα radiation, $\lambda = 1.54056$ Å). A JEOL JEM 2010 transmission electron microscope (TEM) at an accelerating voltage of 200 kV was used to examine the particles morphology. Additionally, high-resolution transmission electron microscopy (HR-TEM) images and selected area electron diffraction (SAED) patterns were taken to determine the nanocrystal structure. Thermogravimetric analyses (TGA) were performed in both air and argon at a heating rate of 2 °C/min up to 600 °C using a SDTQ600 analyzer. The NMR studies were performed on a Varian Gemini-300 spectrometer. FT-IR spectra were obtained on a Perkin-Elmer 1600 spectrometer.

Results and Discussion

In our earlier studies on the synthesis of nanocrystalline spinel-structured oxides, we have found that diethylene glycol is a convenient reaction medium[11] due to its useful physical and chemical properties.[12] This solvent was also used by C. Feldmann et al.[5] for the synthesis of metal oxides with crystal sizes ranging from 30 to 300 nm. The high boiling point (245 °C) of this solvent makes it suitable for variable-temperature syntheses, which is desirable for controlling the rate of reaction and also for obtaining products with improved crystallinity. Diethylene glycol has high permittivity ($\epsilon = 32$), enabling it to dissolve highly polar inorganic and a variety of organic compounds and also to promote reactions whose pathways run through highly polar or ionic intermediates.

As we found previously, the chelating ability of DEG inhibits the formation of metal hydroxides/oxides in solutions containing stoichiometric quantities of transition metal salts and sodium hydroxide.[11] Introduction of a controlled amount of water in these solutions causes hydrolysis of chelated complexes with formation of metal oxides or hydroxides depending on the temperature, with nearly quantitative yield. The structure of complexes existing in solution is not known, but there is evidence that the metal ion coordination sphere contains deprotonated DEG and Cl^- ligands (Figure 1). The rate

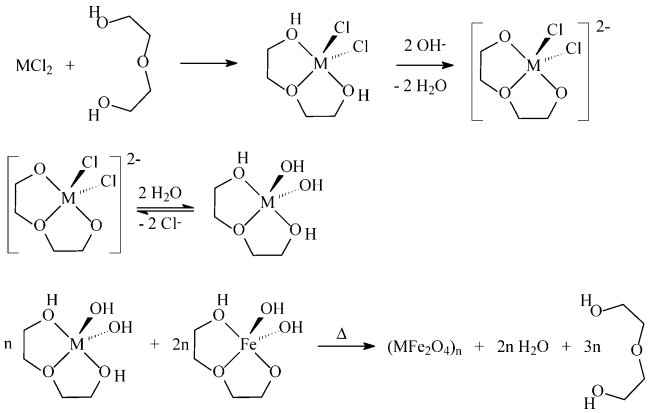

Figure 1. Formation of metal chelated complexes and their decomposition yielding colloidal transition metal ferrites.

of this reaction can be easily controlled by changing the concentration of water and temperature. The course of reaction is monitored visually, and, as the solution turns turbid, the reaction is considered to be complete. In our earlier studies, we next added long-chain carboxylic acids to cap the surface of nanoparticles and isolated them as nanopowders. A series of transition metal ferrites $(MO)_xFe_2O_3$ (M = Mn, Fe, Co, Ni, and Zn; $x = 0.7-1$) with the mean particle sizes ranging from 3 to 7 nm was obtained.[11] In the current study, we addressed the problem of tuning the particle size and the details of the surface chemistry of the nanocrystalline oxides. We focused exclusively on iron ferrite (magnetite) while keeping in mind that our results should apply also to other transition metal ferrites.

Synthesis. To obtain nonaggregated nanoparticles with a chemically active surface, we eliminated the step of capping the nanoparticles with the long-chain carboxylic acid. As a stoichiometric quantity of NaOH (8 equiv) dissolved in DEG is added to the solution containing 1 equiv of $FeCl_2 \cdot 4H_2O$ and 2 equiv of $FeCl_3 \cdot 6H_2O$ dissolved in the same solvent, an immediate color change from yellow to deep green-brown occurs. We explained this[11] in terms of deprotonation of the coordinated alcohol DEG and formation of anionic chelate alkoxide complexes (Figure 1). The resulting solution stays unchanged indefinitely at room temperature if protected from air, but gets oxidized quickly if exposed to air and turns deep yellow. Raising the temperature to 150 °C and then to 210−220 °C causes gradual color change to red-brown and then dark brown with increasing turbidity. As this temperature is maintained for 2 h, a black suspension forms and heating is stopped. After a simple workup procedure using ethanol, the nanopowders are isolated with high yield and tested for their crystal structure and morphology and for reactivity. We performed a series of synthetic experiments varying the rate and time of heating and concentration of the reagents and found no significant difference in the nanocrystals' shape and size with an average value of 5.7 nm (Figure 2a). If the step of aging is shortened to less than 1 h, the quality of the nanocrystals is low, no lattice fringes can be seen, and the edges are diffuse. Our attempts to obtain larger particles by injecting an additional quantity of the reaction solution in the hot solution of the seed nanoparticles yielded a product with wider size distribution. This result indicated that nucleation and growth occurred at a similar rate.

(11) Caruntu, D.; Remond, Y.; Chou, N. H.; Jun, M. J.; Caruntu, G.; He, J.; Goloverda, G.; O'Connor, C. J.; Kolesnichenko, V. *Inorg. Chem.* **2002**, *41*, 6137.

(12) Sobota, P.; Utko, J.; Sztajnowska, K.; Jerzykiewicz, L. B. *New J. Chem.* **1998**, *22*, 851.

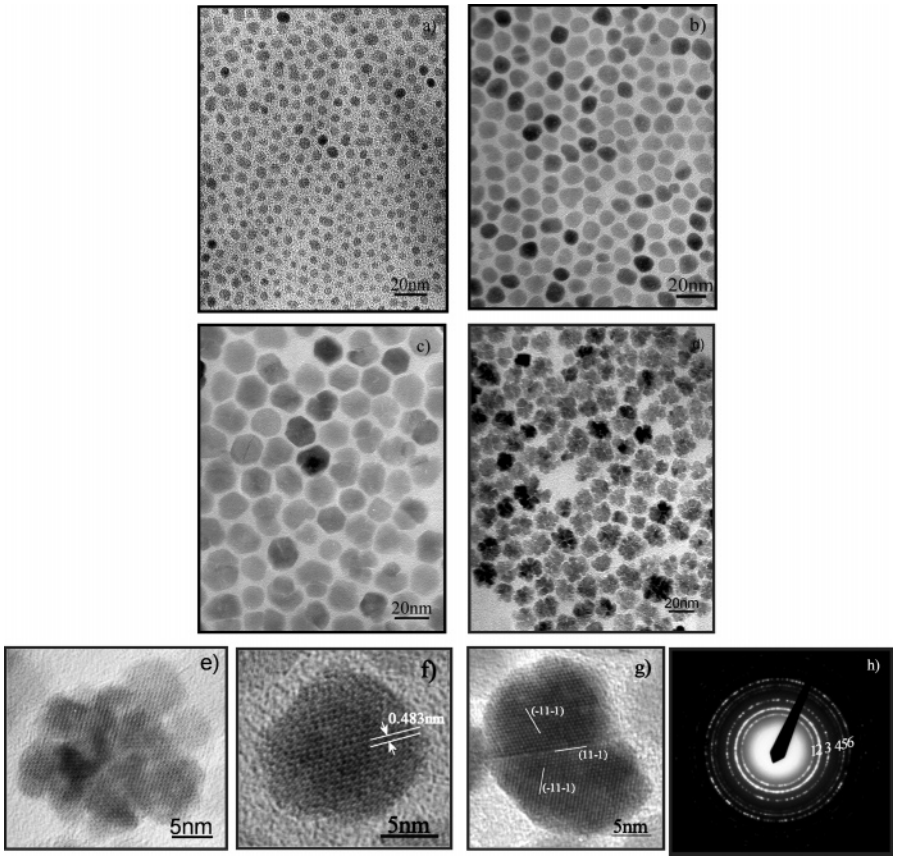

Figure 2. TEM bright field images of the oleate-coated Fe_3O_4 nanoparticles obtained from (a) DEG, (b) a mixture of DEG and NMDEA, and (c) NMDEA; (d) a mixture of DEG and NMDEA at the initial phase of synthesis, and (e) corresponding HRTEM of a typical agglomerate; (f) HRTEM image of a single 12.8 nm-sized Fe_3O_4 nanoparticle viewed along the [10-1] zone axis; (g) HRTEM of a twinned Fe_3O_4 nanoparticle obtained from neat NMDEA; and (h) SAED pattern of Fe_3O_4 nanoparticles prepared from the mixture of DEG and NMDEA.

In the method developed by C. Feldmann et al.,[5] DEG is also used as a coordinating solvent for synthesis of the nanocrystalline metal oxides. According to this method, hydrolysis is accomplished by using easily hydrolyzable metal containing precursors (acetates, acetylacetonates, alkoxides, etc.) and the excess of water. The resulting nanocrystals have much larger sizes (30−300 nm) than the nanocrystals obtained by our method (5.7 nm), which is rather expected, because of the different conditions and the nature of the reacting species.

The results show that under various conditions the particle morphology did not change significantly and prompted us to increase the complexing strength of the reaction medium. Such a change might provide a better control over the rate of hydrolysis of metal chelates, help to stabilize colloids, and therefore obtain larger nanocrystals. The thermal decomposition of triethanolamine-based chelated complexes of iron, cobalt, and nickel in aqueous solution at 250 °C (hydrothermal synthesis) has been used to synthesize corresponding oxides as micrometer-sized crystals.[13] We chose to use diethanolamine, a compound related to both triethanolamine and DEG and whose complexing and chelating properties are well-established.[14] Because diethanolamine has hydrogen bonding more extended than DEG, its physical properties are substantially different, and it has higher viscosity and boiling point. *N*-Methyl diethanolamine (NMDEA), on the other hand, has physical properties similar to those of DEG but complexing properties similar to those of diethanolamine. We performed a series of syntheses of nanocrystalline magnetite in neat NMDEA and in its 1:1 mixture with DEG while keeping all other parameters unchanged.

As a stoichiometric quantity of NaOH (8 equiv) dissolved in a 1:1 DEG/NMDEA solvent mixture is added to a solution containing 1 equiv of $FeCl_2 \cdot 4H_2O$ and 2 equiv of $FeCl_3 \cdot 6H_2O$ dissolved in the same solvent, the color changes from green-brown to green immediately. After exposure at 210−220 °C for 5−10 min, the solution becomes dark green-brown while remaining transparent for at least another 5 min, after which slight turbidity becomes noticeable. In contrast, turbidity appears at 150−160 °C in DEG-solution systems.

The progress of crystallization was monitored by taking aliquots of solution at different time intervals, beginning 5 min after reaching the temperature of 210 °C. The TEM tests at early times showed 11−16 nm agglomerates formed from small (4−6 nm) nanoparticles (Figure 2d). High-resolution images clearly showed

(13) (a) Sapieszko, R. S.; Matijevic, E. *J. Colloid Interface Sci*. **1980**, *74*, 405. (b) Sapieszko, R. S.; Matijevic, E. *Corrosion* **1980**, *36*, 522.

(14) (a) Crans, D. C.; Shin, P. K. *J. Am. Chem. Soc*. **1994**, *116*, 1305. (b) Saalfrank, R. W.; Bernt, I.; Chowdhry, M. M.; Hampel, F.; Vaughan, G. B. M. *Chem.-Eur. J*. **2001**, *7*, 2765. (c) Vinogradova, E. A.; Kokozay, V. N.; Vassilyeva, O. Yu.; Skelton, B. W. *Acta Crystallogr., Sect. E* **2003**, *E59*, m148. (d) Hubert-Pfalzgraf, L. G. *Inorg. Chem. Commun*. **2003**, *6*, 102.

lattice fringes on many of these agglomerates (Figure 2e). Remarkably, the fringes were aligned within many agglomerates. As annealing is continued at 210−220 °C for 2−3 h, the initial shapeless solid formations gradually converted into compact nanocrystals with an average size of 12.7 nm and a well-developed crystal lattice (Figure 2b,f).

Reactions in neat NMDEA solvent, maintained under the same conditions as the mixed solvent system, showed similar behavior. As expected, reactions in this medium produced the largest nanocrystals (16.8 nm). While the smaller nanocrystals have spheroidal shape, the larger ones are faceted. The shape of a small number of nanocrystals indicates they formed by fusion of two or more nanoparticles (Figure 2c).

Therefore, there is a substantial difference in the course of reactions in solutions of DEG and NMDEA. Hydrolysis reactions in DEG followed by nanocrystal nucleation and growth occur with high rate. Aging of the resulting colloids causes internal recrystallization of the nanoparticles without any significant mass transport. This result suggests that formation of metal oxides from chelated DEG complexes is irreversible. In contrast, hydrolysis reactions of metal chelates in solutions containing NMDEA occur at higher temperature and with slower rate. The initially formed small nanoparticles (4−6 nm) quickly agglomerate into 11−16 nm sized aggregates, which then undergo slow recrystallization to produce secondary nanocrystals with a size of 12.7 nm in 1:1 DEG/NMDEA or 16.8 nm in pure NMDEA. Because this recrystallization is accompanied by significant mass transport, this step probably involves an equilibrium between solid oxide and metal complexes in solution. Coalescence of small nanocrystals followed by recrystallization and formation of the larger ones has been found in many colloidal systems with metal oxides.[15] We did not obtain any evidence that coalescence takes place in our DEG-based systems; however, we cannot exclude this happening on the subnanometer level.

Crystal Structure and Morphology of Magnetite Nanoparticles. The structure and phase purity of Fe_3O_4 nanoparticles with various sizes were investigated by powder X-ray diffractometry (XRD). Figure 3 shows the X-ray diffraction patterns of the nanopowders obtained from (a) neat DEG, (b) a mixture of DEG and NMDEA (1:1, w/w), and (c) neat NMDEA. The patterns were found to match well with that of cubic crystalline bulk magnetite (JCPDS file No. 19-629) with no other secondary iron oxide phases. The corresponding values of the refined lattice parameter, 8.419(3), 8.381(7), and 8.388(6) Å, are in good agreement with the value reported for the bulk substance (8.396 Å).[16] The peak broadening of the studied powders decreases from (a) to (c), which is indicative of the nanocrystalline nature of the materials. The crystallite size was estimated from

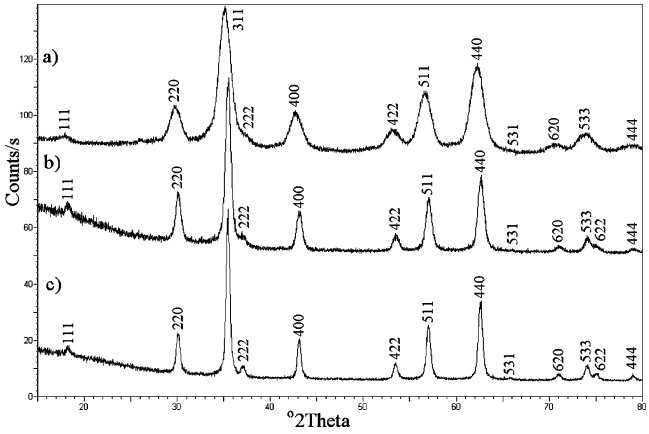

Figure 3. Powder X-ray diffraction patterns of the nanopowders obtained from (a) neat DEG, (b) mixture of DEG and NMDEA, and (c) neat NMDEA.

the six most intense peaks of each X-ray diffraction pattern using Scherrer's formula;[17] the calculated average values are (a) 6.4 nm, (b) 12.3 nm, and (c) 17.4 nm.

Details about the structure and morphology of the obtained nanoparticles were provided by TEM studies. Figure 2a−d shows the TEM micrographs of different-sized Fe_3O_4 nanoparticles. The nanocrystals are clearly separated from each other in monolayers, and their shape changes with increasing size from almost spherical (a) to hexagonal (d). The average sizes were estimated to be (a) 5.7 nm, (b) 12.7 nm, and (c) 16.8 nm with corresponding standard deviation values (δ) of 16.2%, 8.8%, and 11.5% (Figure 4). The sizes of the nanocrystals determined by TEM were in good agreement with the size calculated from peak broadening in X-ray diffractograms, indicating that most of the nanoparticles are single-crystalline.

The SAED pattern (Figure 2h), taken from a monolayer of 12.7 nm-sized Fe_3O_4 nanoparticles, contains six well-defined spotted rings. As anticipated, the spotted appearance of the diffraction rings is due to high crystallinity of the obtained nanoparticles. The corresponding interplanar spacings calculated from the SAED pattern are presented in Table 1. The values obtained are consistent with those obtained from the X-ray diffraction pattern, as well as those corresponding to standard bulk Fe_3O_4 (JCPDS file No. 19-629).[18]

The HRTEM image of a typical 12.7 nm-sized Fe_3O_4 nanoparticle is presented in Figure 2f. The micrograph reveals highly ordered lattice fringes with a fringe separation of 4.83 Å, which corresponds to {111} lattice planes. This value agrees well with that of 4.85 Å determined from the analysis of the XRD pattern. Although most of the nanoparticles are single-crystalline, a small number of twinned nanocrystals were also observed (Figure 2g), supporting coalescence of the primary particles as one of the steps in their crystallization.

Surface of Magnetite Nanoparticles. A thermogravimetric study of the magnetite nanoparticles obtained from DEG and NMDEA solutions was performed over the range of temperature 20−600 °C in air and

(15) (a) Pen, L. R.; Banfield, J. *Am. Mineral.* **1998**, *83*, 1077. (b) Banfield, J. F.; Welch, S. A.; Zhang, H.; Tomsen-Ebert, T.; Penn, L. R. *Science* **2000**, *289*, 751. (c) Leite, E. R.; Giraldi, T. R.; Pontes, F. M. *Acta Microscopica* **2003**, *12* (C), 325. (d) Pacholski, C.; Kornowski, A.; Weller, H. *Angew. Chem., Int. Ed.* **2002**, *41*, 1188. (e) Park, J.; Privman, V.; Matijević, E. *J. Phys. Chem.* **2001**, *105*, 11630. (f) Morales, M. P.; Gonzalez-Carreno, T.; Serna, C. J. *J. Mater. Res.* **1992**, *7*, 2538.

(16) Cornell, R. M.; Schwertmann, U. *The Iron Oxides: Structure, Properties, Reactions, Occurrence and Uses*; VCH: New York, 1996; p 28.

(17) West, A. R. *Solid State Chemistry And Its Applications*; John Wiley & Sons: London, 1984; p 174.

(18) Ma, M.; Zhang, Y.; Yu, W.; Shen, H.; Zhang, H.; Gu, N. *Colloids Surf., A* **2003**, *212*, 3190226.

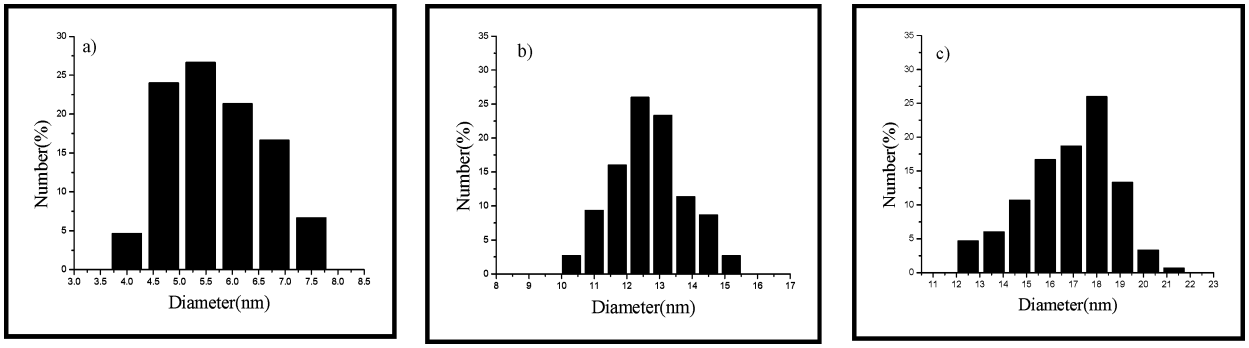

Figure 4. Particle size histograms of Fe_3O_4 nanoparticles prepared from (a) neat DEG, (b) mixture of DEG and NMDEA, and (c) neat NMDEA.

Table 1. Interplanar Spacings, *d* (Å), Deduced from the Analysis of SAED and XRD Patterns and the Values Corresponding to Standard Bulk Magnetite

	diffraction ring					
	1	2	3	4	5	6
SAED	3.089	2.624	2.194	1.784	1.694	1.550
XRD (Figure 3b)	2.965	2.526	2.095	1.710	1.613	1.481
XRD (standard bulk Fe_3O_4)	2.967	2.532	2.099	1.714	1.615	1.484
hkl	220	311	400	422	511	440

argon atmosphere. The first and brief event of weight loss occurs below 100 °C and is due to evaporation of the adsorbed solvent. The TGA curves corresponding to the runs in air show a weight gain effect between 125 and 175 °C. The FT-IR spectrum (in the range of Fe−O vibrations) of the nanopowder exposed to air at 210 °C evidenced that this weight gain is attributed to the oxidation of Fe_3O_4 to Fe_2O_3. Regardless of the atmosphere, the main weight loss starts at ~175 °C and ends at ~ 325 °C when the rate of heating is 2 deg/min. The value of the total mass change correlated with particle size: it was larger for smaller particles (6.75% for 5.7 nm) and smaller for the larger ones (4.08% for 12.7 nm and 1.36% for 16.8 nm). A typical TGA curve corresponding to the run in air and representing the 16.8 nm nanocrystals is shown in Figure 5. The residues after decomposition of the samples in air at the temperature 600 °C were identified by X-ray diffractometry as α-Fe_2O_3. The observed weight loss is due to evaporation of the adsorbed DEG, NMDEA, and water from the surface of nanoparticles, as well as to dehydration of the surface OH-groups.

We attempted to characterize the composition of the surface by IR spectroscopy, but the quality of the spectra was unsatisfactory due to a low concentration of organic component. To solve this problem, we used destructive methods to separate the organic and inorganic constituents and then used ^{1}H NMR spectrometry for identification of the organic component and determination of its content semiquantitatively by integration. Exact quantities of nanopowder and deuterium oxide were sealed in an ampule and heated at 100 °C to extract the organic constituent into solution and facilitate coagulation of iron oxide. After heating for ~1 h, the ampule was opened and the resulting clear colorless solution was separated, weighed, and transferred into an NMR tube. A measured quantity of DMSO was added as a standard for integration. The sample synthesized from DEG solution revealed only DEG and DMSO peaks in its proton spectrum (Figure 6). The content of DEG in the

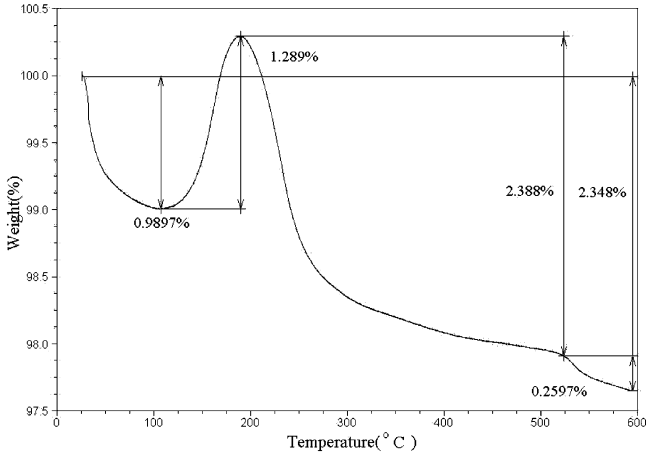

Figure 5. TGA curve for the uncapped 16.8 nm magnetite nanoparticles.

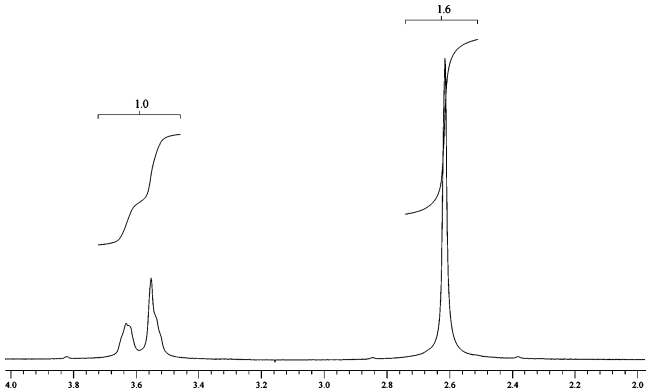

Figure 6. ^{1}H NMR spectrum of the product of decomposition of Fe_3O_4 nanoparticles in D_2O solution. Peak at 2.61 ppm represents DMSO added as a standard for integration.

nanopowders determined by integration was 2.9 wt %, indicating that DEG is not merely a contaminant, but a constituent.

Decomposition of the magnetite samples synthesized in the systems containing NMDEA required harsher conditions. NMR tests of the organic residues revealed that NMDEA decomposes under these conditions yielding a mixture of unidentified compounds.

As it was determined by TGA and ^{1}H NMR, all nanocrystalline magnetite products contained different quantities of adsorbed volatile constituents, more for smaller nanocrystals and less for larger ones. These substances were identified as diethylene glycol and the decomposition products of *N*-methyl diethanolamine.

Nanocrystals' Surface Reactivity and Dispersibility. The reactivity of the obtained nanocrystalline magnetite products was tested using their reaction with oleic acid in toluene solution. This test was based on the ability of inorganic nanocrystals capped with long-chain carboxylates to form colloids in hydrocarbons. Additional examination of their ability for repeated colloid formation after precipitation may be used for testing how strongly the capping ligand is bound to the nanocrystal surface. The nanopowders synthesized from DEG or NMDEA/DEG solutions exhibited high reactivity, dissolving at room temperature or after short refluxing. Addition of methanol to the resulting dispersions caused precipitation of solids that were separated, washed with methanol, and tested for solubility in toluene. We determined that DEG-derived nanopowders could be redispersed in toluene, whether refluxing was used when they reacted with oleic acid. However, oleate-capped nanocrystals originating from DEG/NMDEA lost their dispersibility if refluxing was not used when they were reacted with oleic acid. As refluxing was used, the solids remained dispersible in toluene. Magnetite samples synthesized using neat NMDEA were always the least reactive. Their complete dissolution in toluene/oleic acid solution could not be achieved even after prolonged refluxing.

Analysis of the surface showed that all nanocrystals contain organic compounds, either DEG or NMDEA or both. It is not clear how these molecules are bound to the nanocrystal surface, although it is likely they partially use their chelating properties. Evidently, these organic constituents play the essential role in protecting the nanocrystals against agglomeration and, consequently, in their surface reactivity and dispersibility.

It is likely that when the DEG-containing nanopowders react with oleic acid, the carboxyl group binds directly to the surface metal ions, replacing DEG molecules. This chemical bonding provides stability and dispersibility, and, as we observed, the capping ligand cannot be removed by washing. The products of synthesis from NMDEA contain basic amine functions on the surface of nanocrystals, which changes their reactivity with carboxylic acids. It is likely that at room temperature the interaction is limited to the formation of hydrogen bonds between carboxylic and amino groups. Oleic acid adsorbed via hydrogen bonding can be easily removed by washing with alcohols. At an elevated temperature and in the presence of an excess of oleic acid, the final product contains oleate ligand covalently bound to the surface of nanocrystals similar to the ones obtained from DEG. The presence of oleate anions in the samples was confirmed by IR spectroscopy: the spectra exhibited bands corresponding to the stretching vibrations of C−H bonds at 2920 and 2850 cm^{-1} and of carboxylic groups at 1540 and 1455 cm^{-1}.

The isolated nanocrystalline magnetite was tested for dispersibility in methanol and water. Most of the tested samples could be dispersed in pure solvents; however, the dissolution was dramatically facilitated by the presence of traces of mineral or carboxylic acids. Colloidal solutions of 12.7 nm nanoparticles were obtained with concentrations as high as 6.0 mg/mL in water and 4.6 mg/mL in methanol. Acidification not only improved dispersing, but also caused great stabilization: both aqueous and methanol colloids containing ~75 μmol/L of HCl were indefinitely stable. The TEM examination of aqueous colloids aged for 3 months revealed their nonaggregated nature (Figure 7).

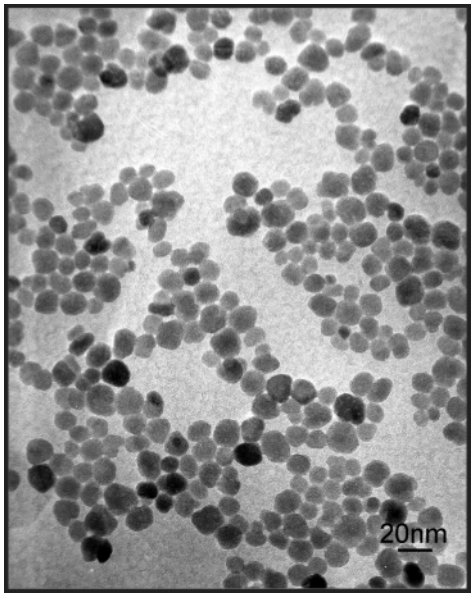

Figure 7. TEM micrograph of Fe_3O_4 nanoparticles dispersed in water; the aqueous dispersion was aged for 3 months.

Conclusion

The high-yield synthesis of the uncapped nanocrystals of Fe_3O_4 with chemically active surfaces is accomplished by the elevated-temperature hydrolysis of chelate iron alkoxide complexes in solutions of diethylene glycol and *N*-methyl diethanolamine. The rate of this reaction is easily controlled by changing the temperature and concentration of the reactants, and high yield is obtained due to the practically irreversible hydrolysis. The highly polar medium of alcohol and byproduct ions (Na^+, Cl^-) stabilizes the colloids, which is essential for the nucleation and growth steps. As the stability of these colloids becomes exhausted, the oxides precipitate as nanopowders whose surface is passivated by a labile layer of the adsorbed solvent. The different donor properties of diethylene glycol and *N*-methyl diethanolamine affect the rate of hydrolysis and crystallization and, therefore, the final size of the nanocrystals. The smallest (5.7 nm) and largest (16.8 nm) nanocrystals were obtained in the former and the latter solvents, respectively. Nanocrystals of intermediate size (12.7 nm) were obtained in a 1:1 mixture of the two solvents. By varying the solvent ratio, one may probably synthesize Fe_3O_4 nanocrystals of intermediate sizes, and this method may be applicable for the synthesis of other nanocrystalline metal oxides with chemically active surface. The isolated nanocrystalline powders are easily dispersible in toluene in the presence of oleic acid and in water or methanol without using a surfactant. This property of the nanoscaled magnetite, as a biologically compatible magnetic material, may promote its application in biology and medicine as a component for diagnostic and therapeutic tools. A study of the reactivity of these nanocrystals with various bifunctional organic molecules is in progress.

Acknowledgment. This work is supported by DARPA grant MDA972-02-1-001. We wish to thank Jinke Tang for his help with XRD experiments and Bryan Klassen for his help with the preparation of this manuscript.

CM0487977